Testing fuel cell catalysts under more realistic reaction conditions: accelerated stress tests in a gas diffusion electrode setup

Shima Alinejad[a], Masanori Inaba[b,c], Johanna Schröder[a], Jia Du[a], Jonathan Quinson[b], Alessandro Zana[a] and Matthias Arenz[a*]

[a]Department of Chemistry and Biochemistry, University of Bern, Freiestrasse 3, CH-3012 Bern, Switzerland

[b]Department of Chemistry, University of Copenhagen, Universitetsparken 5, DK-2100 Copenhagen Ø, Denmark

[c]Toyota Central R&D Labs., Inc., Nagakute, Aichi 480-1192, Japan

*Corresponding author

University of Bern, Freiestrasse 3, CH-3012 Bern, Switzerland

Phone: +41 31 631 53 84

Email: matthias.arenz@dcb.unibe.ch

Abstract

Gas diffusion electrodes (GDE) setups have very recently received increasing attention

as a fast and straight-forward tool for testing the oxygen reduction reaction (ORR) activity of surface area proton exchange membrane fuel cell (PEMFC) catalysts under more realistic reaction conditions. In the work presented here, we demonstrate that our recently introduced GDE setup is suitable for benchmarking *the stability* of PEMFC catalysts as well. Based on the obtained results, it is argued that the GDE setup offers inherent advantages for accelerated degradation tests (ADT) over classical three electrode setups using liquid electrolyte. Instead of the solid-liquid electrolyte interface in classical electrochemical cells, in the GDE setup a realistic three-phase boundary of (humidified) reactant gas, proton exchange polymer (e.g. Nafion) and the electrocatalyst is formed. Therefore, the GDE setup not only allows accurate potential control but also independent control over the reactant atmosphere, humidity and temperature. In addition, the identical location transmission electron microscopy (IL-TEM) technique can easily be adopted into the setup enabling a combination of benchmarking with mechanistic studies.

Keywords

Accelerated stress tests; Gas Diffusion Electrode; Platinum; Carbon Supported High Surface Area Catalysts; Fuel Cells;

1. Introduction

Benchmarking activity and stability of proton exchange membrane fuel cell (PEMFC) catalysts using classical three-electrode setups and aqueous electrolyte solution is a popular approach [1, 2]. The electrode potential can be controlled independent of the reaction conditions allowing not only to compare the performance of different PEMFC catalysts, but also to investigate how potential excursions affect the catalyst stability and the degradation mechanism. For the latter, accelerated degradation tests (ADTs) are employed in combination with techniques such as identical location transmission and scanning electron microscopy (IL-TEM and IL-SEM) [3-12] and scanning flow cells (SFC) coupled to inductively coupled plasma - mass spectrometry (ICP-MS) [13, 14]. Thus, degradation mechanisms such as metal dissolution and particle detachment can be related to certain excursions in the electrode potential as well as catalyst properties such as particle size, carbon support, etc. The aim of ADTs thereby is to apply realistic conditions and at the same time to reduce the time in which a performance loss is observed significantly [15-17]. Although this is a contradictory goal, certain ADT protocols are commonly accepted as a compromise, in particular the one of the Fuel Cell Commercialization Conference of Japan (FCCJ) [18, 19] simulating load-cycle and start-up/shutdown conditions of a proton exchange membrane fuel cell (PEMFC).

Despite the achievements made, the current approach also has disadvantages. For example, it is not clear if and how an aqueous electrolyte environment as compared to a realistic three-phase boundary of humidified reactant gas (proton exchange polymer, e.g. Nafion) influences the degradation of the active component and the carbon support, respectively. In aqueous electrolyte environment it is found that for certain Pt/C fuel cell catalysts and simulated start-up/shutdown conditions the degradation mechanism is restricted to particle loss, most likely due to carbon corrosion [3]. However, at simulated load cycle conditions the main observed degradation mechanism changes to particle migration and coalescence [20]. By comparison, in membrane electrode assembly (MEA) tests the reported degradation mechanism is in general platinum dissolution [21], and in some cases extensive carbon corrosion. More subtle mechanisms such as particle migration and coalescence cannot be identified.

Only few efforts exist to combine a simple setup with a more realistic environment [22-29]. Here we demonstrate how our recently introduced gas diffusion electrode (GDE) setup [30-32] can be used for benchmarking the stability of high surface PEMFC catalysts under realistic reaction conditions. Gas diffusion electrode setups have very recently received increasing attention allowing to combine the ease of use known from electrochemical three-electrode setups and liquid aqueous environment with reaction

conditions closer to applications [33]. In the work presented, it is shown that in the GDE setup parameters such as the reactant gas atmosphere and its humidity can be easily controlled and their influence on the catalyst stability be studied. Thus, the setup offers inherent advantages over the conventional three-electrode setups for ADTs. In addition, the IL-TEM technique can easily be adopted into the setup enabling a combination of stability benchmarking with mechanistic studies.

2. Experimental

2.1. Chemicals, materials, and gases.

Ultrapure water (resistivity > 18.2 MΩ·cm, total organic carbon (TOC) < 5 ppb) from a Milli-Q system (Millipore) was used for acid/base dilutions, catalyst ink formulation, and the GDE cell cleaning. The following chemicals were used in ink formulation and electrolyte preparation: Isopropanol (IPA, 99.7+ %, Alfa Aesar), 70 % perchloric acid ($HClO_4$, suprapure, Merck), potassium hydroxide hydrate ($KOH·H_2O$, Suprapur, Merck), commercial Pt/C catalysts (46.0 wt. % TEC10E50E and 50.6 wt. % TEC10E50E-HT, Tanaka kikinzoku kogyo as well as HISPEC 3000, Johnson Matthey), and Nafion dispersion (D1021, 10 wt. %, EW 1100, Fuel Cell Store). A Nafion membrane (Nafion 117, 183 µm thick, Fuel Cell Store) and a gas diffusion layer (GDL) with a microporous layer (MPL) (Sigracet 39BC, 325 µm thick, Fuel Cell Store) were

90 employed in the GDE cell measurements. Before use, the Nafion membrane was
91 prepared and activated as follows: after cutting several circles with a diameter of 2 cm
92 from a sheet of Nafion membrane, the membranes were treated for 30 minutes at 80 °C
93 in 5 wt.% H_2O_2, followed by rinsing with Milli-Q water. Then, the membranes were
94 treated for 30 minutes at 80 °C in Milli-Q water followed by rinsing with Milli-Q water.
95 Finally, the membrane was treated for 30 minutes at 80 °C in 8 wt.% H_2SO_4, again
96 followed by a rinsing with Milli-Q water. All membranes were kept in a glass vial filled
97 with Milli-Q water. The following gases from Air Liquide were used in electrochemical
98 measurements: Ar (99.999 %), O_2 (99.999 %), and CO (99.97 %). TEM characterization
99 of the respective Pt/C catalysts can be found in the supporting information (FigureS1).

100 *2.2. Gas Diffusion Electrode cell setup.*

101 An in-house developed GDE cell setup was employed in all electrochemical
102 measurements that was initially designed for measurements in hot phosphoric acid [24].
103 The design used in the present study has been described before [31]. In short, it was
104 optimized to low temperature PEMFC conditions (< 100 °C) by placing a Nafion
105 membrane between catalyst layer and liquid electrolyte; no liquid electrolyte is in direct
106 contact with the catalyst [31]. A photo of the parts of the improved GDE setup is shown
107 in Figure 1.

The cell body above the Nafion membrane is made of polytetrafluoroethylene (PTFE). A platinum mesh and a reversible hydrogen electrode (RHE) were used as a counter electrode (CE) and a reference electrode (RE), respectively. The counter electrode placed inside of a glass capillary tube with a glass frit on the bottom, which avoids the trapping of gas bubbles in the hole of the Teflon cell and consequently helps increasing the reproducibility of the measurement. All potentials in this study are referred to the RHE potential. For initial cleaning, the Teflon upper part was soaked in mixed acid (H_2SO_4:HNO_3 = 1:1, v:v) overnight. Subsequently it was rinsed thoroughly by ultrapure water, and boiled in ultrapure water twice. Between the measurements the Teflon upper part was boiled in ultrapure water twice.

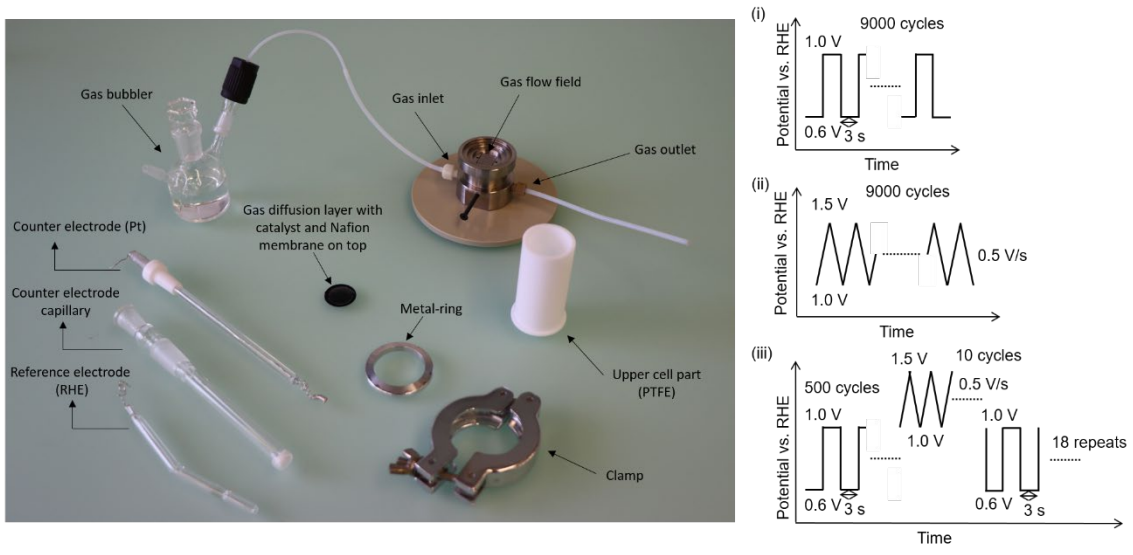

Figure 1. Photo of the individual components of the GDE cell employed in the present study (left) and different applied ADT protocols (right). The Nafion membrane and the GDL (including the catalyst layer fabricated on it) are sandwiched between the upper and lower cell body. The upper cell body is pressed to the lower cell body by a metal

123 ring and a clamp. A gas humidifier (gas bubbler) is connected to the reactant gas. The
124 counter electrode is inserted into a glass capillary to avoid gas capture at the Teflon cell.
125 Optionally, instead of applying a catalyst layer on the GDL an Au-TEM grid with a thin
126 catalyst layer can be sandwiched between GDL and Nafion membrane (not shown). The
127 ADT protocols are simulating (i) load cycles, (ii) start-up/shutdown conditions, and (iii)
128 a combination of both.

129

130 *2.3. Catalyst ink formulation and catalyst layer application.*

131 2.0 mg of the respective commercial 46.5 wt. % Pt/C catalyst powder and 10.09 µL (or
132 9,36 µL) of the 10 wt. % Nafion dispersion were mixed with 4.74 mL (or 5.15 mL) of
133 IPA:ultrapure water (1:3, v:v) mixed solvent. The glass vial containing the mixture was
134 placed in the ultrasonic bath and sonicated for 15 minutes. Subsequently the mixture
135 was dispersed using a horn sonicator (Q500, QSonica) for 1 minute. Before the
136 application of the catalyst ink on the GDL, circular pieces (φ = 20 mm) of the GDL
137 were punched from a larger sheet. The catalyst ink was sprayed onto the GDL (MPL
138 coated side) by using a pump (Harvard apparatus 11 plus) with a flow rate of 0.5
139 mL/min and an ultrasonic spray nozzle (Sonozap narrow spray atomizer). During the
140 spraying, the catalyst ink was constantly sonicated by an ultra sonicator (Sonozap
141 ultrasonic atomizer) with a power of 1.5 W and frequency of 130 KHz and the GDL was
142 heated on a heating plate (140 °C) and covered with an iron mask so that a circular
143 catalyst layer (φ = 3 mm) was formed at the center of the GDL.

144 *2.4. Electrochemical measurements.*

145 The electrochemical measurements were performed using a computer controlled
146 potentiostat (ECi 200, Nordic Electrochemistry). The measurements were performed
147 with 4 M $HClO_4$ aqueous solution in the upper Teflon compartment of the GDE setup
148 applying different temperatures as reported previously [31]. Prior to the measurements,
149 the electrode was purged from the backside (through the gas diffusion layer) with Ar gas
150 and the catalyst was cleaned by potential cycles between 0.06 and 1.10 V_{RHE} at a scan
151 rate of 500 mV s^{-1} until a stable cyclic voltammogram could be observed (ca. 50 cycles).
152 The resistance between the working and reference electrode (~10 Ω) was compensated
153 to effective value of around 1 Ω by using analog positive feedback scheme of the
154 potentiostat. The resistance was determined online using an AC signal (5 kHz, 5 mV)
155 [34].

156 To determine the stability of the Pt/C electrocatalysts, ADTs inspired by the Fuel Cell
157 Commercialization Conference of Japan [18] were performed. Three different ADT
158 protocols were tested: (i) a protocol simulating load-cycles, where the electrode
159 potential was modulated with a square wave and stepped between 0.6 and 1.0 V_{RHE} with
160 a holding time of 3 s at each voltage for a total of 9000 potential cycles, (ii) a protocol
161 simulating start-up/shutdown conditions [35], where the electrode potential was cycled

with a scan rate of 0.5 V s^{-1} between 1.0 and 1.5 V_{RHE} for a total of 9000 potential cycles and (iii) a mixed protocol combining (i) and (ii), which consisted of 500 potential cycles of the load-cycling protocol followed by 10 potential cycles of the start-up/shutdown protocol, repeated overall 18 times; in the following we refer to this protocol as mixed protocol. In order to monitor the H_{upd} area and the change of the quinone/hydroquinone (Q/HQ) redox peak [36, 37] after each 1000 potential cycles (500 cycles for procedure (iii)) six cyclic voltammograms were recorded in Ar atmosphere at a scan rate of 0.5 V s^{-1}. The electrochemically active surface area (ECSA) of the catalyst was determined by conducting CO stripping voltammetry before and after the ADT. We did not record further CO stripping during the ADT to minimize the potential negative impact of CO stripping on the surface area [38-40]. For the CO stripping measurements, the working electrode was held at 0.05 V while purging first CO through the GDL for 5 minutes and thereafter Ar for an additional 5 minutes. The ECSA was determined from the CO (Q_{CO}) oxidation charge recorded at a scan rate of 50 mV s^{-1}. Unless otherwise stated, all measurements were performed at room temperature.

2.5. TEM grid preparation.

For IL-TEM investigations, a gold finder grid (400 mesh; Plano, Germany) was used. The catalyst ink was diluted by a factor of 1:10. Afterwards, 10 µL of diluted catalyst

ink were pipetted onto the gold finder grid. In order to avoid overlapping of the catalyst particles, after approximately 10 s the droplet of the catalyst was carefully absorbed off from the grid with a filter paper. Afterwards the grid was dried, and the catalyst investigated in a Technai Spirit (FEI) with an accelerating voltage of 80 kV before and after accelerating degradation test. The TEM grid was placed between a Nafion membrane and a GDL (without a catalyst layer on it) during the ADT. The ADT for the IL-TEM experiment was conducted by applying the load-cycling protocol (1200 cylces) at 60 ˚C, 100 % relative humidity (RH).

3. Results and discussion

3.1. Comparison of different ADT protocols.

The aim of the present study was to employ our recently developed GDE setup mimicking PEMFC environment to ADT studies. At first, we compared different ADT protocols for their suitability to monitor the catalyst degradation in the GDE setup. The different ADT protocols are designed to apply as realistic conditions as possible and at the same time to significantly reduce the time in which a performance loss is observed. For PEMFCs a variety of different ADT protocols can be found in literature, here we tested the popular approach suggested by the Fuel Cell Commercialization Conference

198 of Japan [18, 19] simulating load-cycle and start-up/shutdown conditions, respectively.
199 Load-cycle conditions are simulated by stepping the applied electrode potential between
200 0.6 and 1.0 V_{RHE} and holding the potential for three seconds each. 0.6 V_{RHE} is a typical
201 cell potential under full load, whereas 1.0 V_{RHE} is close to the open circuit potential of
202 Pt and represents the cell voltage at idle conditions. Start-up/shutdown conditions are
203 simulated by scanning the applied electrode potential between 1.0 and 1.5 V_{RHE} with a
204 scan rate of 0.5 V s^{-1}, which simulates an increase in cathode potential when introducing
205 hydrogen in an air filled flowfield or replacing the hydrogen by air during the start-up
206 and shut-down period, respectively [35]. For a better understanding of the ADT
207 protocols the reader is referred to ref. [18]. The total duration of the load-cycle
208 treatment lasted 9000 cycles, which is a total of 16 and 19 hours in Ar and O_2
209 atmosphere, respectively. The degradation is monitored by cyclic voltammograms
210 recorded in Ar atmosphere after each 1000 cycles as well as CO stripping experiments
211 before and after of the ADT protocol (therefore, the total time varies as for the ADT
212 protocol measured in Ar and O_2, respectively, as the O_2 needed to be replaced from the
213 flow field before measuring the cyclic voltammograms). The start-up/shutdown
214 treatment lasted 9000 cycles as well, which is a total of 6 and 9 hours in Ar and O_2
215 atmosphere, respectively.

In Figure 2 the effect of both ADT protocols employed in the GDE setup is demonstrated on a commercial Pt/C catalyst with an average particle size of 2-3 nm, see FigureS1. On the left-hand side, the cyclic voltammograms (CVs) recorded every 1000 cycles in Ar atmosphere are plotted, whereas on the right-hand side the CO stripping curves recorded before and after the ADT treatment are shown. For Pt/C, the ECSA loss can be monitored based on the changes in H_{upd} area in the CVs recorded in Ar atmosphere as well as changes in the area under the CO stripping curves. Further information concerning the degradation of the catalyst can be derived from the change in the "oxide region" (~ 0.75 V_{RHE}) and the formation of a Q/HQ redox peak (~ 0.6 V_{RHE}). As seen in Figure 2 a, b), the behavior of the Pt/C catalyst upon the load cycling treatment (i) is qualitatively the same as reported previously for ADT measurements performed in half-cells with liquid electrolyte [37]. The Pt/C catalyst loses continuously ECSA and the reduction peak in the "oxide region" decreases, whereas its peak potential slightly shifts to higher potentials. After 9000 cycles a total loss in ECSA of 41.5 ± 2.3 % is determined. Interestingly this is roughly 10 % more loss than what is observed for the same catalyst in a conventional cell with liquid electrolyte (32.0 ± 1.6), see Table 1 and FigureS2, 3 for a summary of the ECSA losses observed for different catalysts

234 and under different conditions.

235

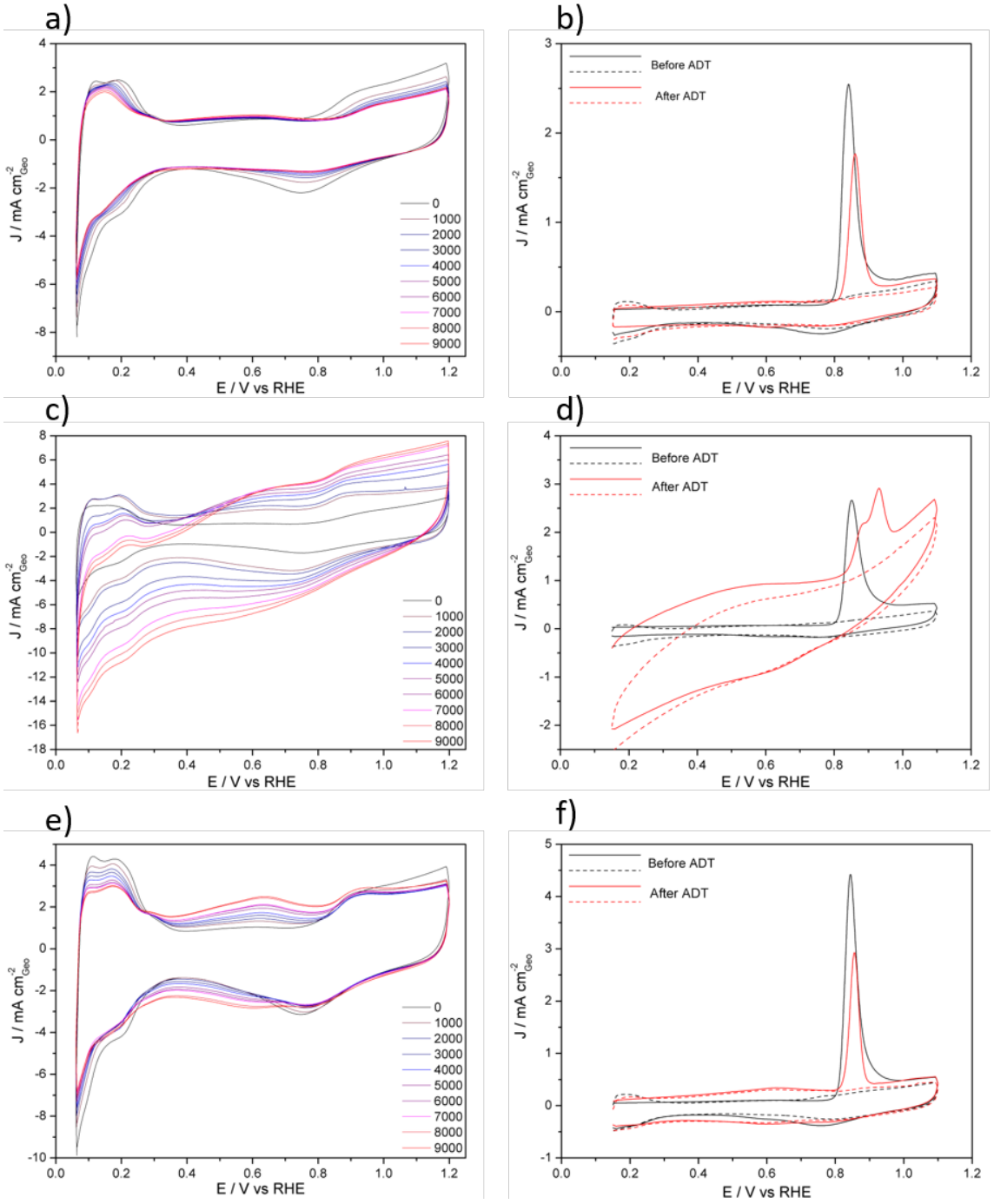

236

237 **Figure 2.** Influence of different ADT protocols performed in Ar atmosphere on the
238 electrochemical behavior of a commercial Pt/C catalyst (TEC10E50E). On the left-hand

side, the cyclic voltammograms (sweep rate 0.5 V s^{-1}) recorded every 1000 cycles in Ar atmosphere are shown, whereas on the right-hand side the initial and final CO stripping curves are shown (solid line) together with the subsequent cyclic voltammogram (solid line); both recorded at a sweep rate of 0.05 V s^{-1}. (a,b) Step protocol simulating load cycles, (c,d) CV protocol simulating start-up/shutdown conditions, (e,f) mixed protocol combining the two prior protocols. The measurements were performed at room temperature.

In contrast to protocol (i), the effect of applying the start-up/shutdown protocol (ii) in the GDE setup is more difficult to compare with previous measurements using conventional half-cells and liquid electrolyte [20, 37, 41]. When applying protocol (ii) in the GDE setup, see Figure 2 c, d), the CVs recorded in Ar atmosphere quickly lose the features of Pt/C and become significantly tilted with time. This indicates massive carbon corrosion and an increase in cell resistance with time, which is confirmed by the online superposition of an AC signal (5 kHz, 5 mV). The same trend is seen in the CO stripping curve recorded after the ADT procedure. Due to the significant distortion of the CVs and CO stripping measurements a proper analysis of the surface area loss from determining the H_{upd} or the CO stripping charge is highly questionable. Most likely the prolonged exposition to high electrode potentials leads to the massive oxidation not only of the catalyst layer, but also the MPL and possibly even the GDL. Note that in our measurements the amount of carbon in the catalyst layer is significantly less than the carbon in the MPL.

A more representative degradation of the catalyst is achieved by the presented mixed ADT protocol (iii), which combines load cycles with start-up/shutdown cycles in a sequence of load cycles and start-up/shutdown events, Figure 2e, f). Although only a limited number of high potential excursions are applied, the evolving features in the CV recorded every 1000 cycles are distinctively different than in the load-cycle protocol (i): i.e., the CVs exhibit a strong increase in double layer capacitance and the formation of a pronounced Q/HQ redox peak is observed. Although also for this ADT, it cannot be excluded that the observed features are related to the degradation of the catalyst layer as well as the MPL and the GDL, the loss in CO stripping area is solely related to the loss in ECSA of the catalyst. In contrast to the commonly applied start-up/shutdown protocol (ii), the measurements from the mixed ADT protocol can be analyzed with confidence and thus we suggest using such a mixed procedure instead of the protocol (ii) proposed by the FCCJ for simulating start-up/shutdown conditions. Despite of the fact that the catalyst experiences only 180 high potential excursions in total, it is seen that in the mixed protocol (iii) the ECSA loss (54.3 ± 0.1 %) is more than 10 % higher than upon applying the load-cycle protocol (i) (41.5 ± 2.3 %), see Table 1.

3.2. The influence of the particle size and heat treatment.

279 We performed the same measurements (ADT protocol (i) and protocol (iii)), on an
280 additional commercial catalyst (TEC10E50E-HT) with larger particle size, i.e. ca. 4-5
281 nm instead of 2-3 nm, see FigureS1. As expected and shown previously in ADT using
282 conventional electrochemical cells [42], the results obtained in the GDE setup
283 demonstrate a significantly higher loss in ECSA for the catalyst with smaller particle
284 size (2-3 nm, TEC10E50E) than for the one with larger particle size (4-5 nm,
285 TEC10E50E-HT). Upon applying the load cycling protocol (i) using the Pt/C catalyst
286 with 4-5 nm particle size, the ECSA loss is 19.2 ± 0.5 %, i.e. it is reduced to less than
287 half as compared to the Pt/C with 2-3 nm particle size (ECSA loss of 41.5 ± 2.3 %).
288 Applying the mixed protocol (iii) the stability improvement is even more significant, i.e.
289 an ECSA loss of 20.7 ± 0.4 % is detected as compared to 54.3 ± 0.1 %. An obvious
290 explanation for the observed stability improvement is the larger particle size of the
291 active Pt phase. It should be mentioned however, that the particle size might not the
292 only contributing factor to the enhanced stability. As these are commercial samples, the
293 exact synthesis routes are not publicly available, the catalyst notation however, suggests
294 that the larger particle size results from a heat treatment of the Pt/C catalyst with 2-3 nm
295 particle size. Such treatments result not only in increased particle sizes due to
296 agglomeration and sintering, but also influence the carbon support properties [43]. For a

297 more detailed study of the influence of the particle size on the catalyst stability, which is
298 not the scope of this work, therefore, the use of in-house synthesized catalysts using the
299 toolbox approach [44] is suggested.

300 *3.3. The influence of the reactant gas conditions.*

301 Above discussed ADT measurements were performed under Ar atmosphere. Performing
302 the same measurements in O_2 atmosphere using the Pt/C catalyst with 2-3 nm particle
303 size, leads to small but distinctive differences, see Figure 3. The startup/shutdown
304 protocol (ii) faces the same limitations as when performed in Ar atmosphere and is
305 therefore not discussed further. However, in the CVs of the load-cycle protocol (i), it
306 can be seen that (as compared to the ADT protocol (i) performed in Ar atmosphere) the
307 formation of the Q/HQ redox peak is more pronounced indicating an impact of the O_2
308 atmosphere on the carbon support oxidation. This is confirmed in the CO stripping
309 measurements, where a small, but distinctive difference in ECSA loss is seen whether
310 the ADT protocol is performed in Ar (41.5 ± 2.3 %) or O_2 (48.1 ± 1.6 %) atmosphere.
311 Interestingly the difference in ECSA loss between measurements performed in Ar and
312 O_2 atmosphere is less pronounced applying the mixed ADT protocol (iii). This finding
313 might be related to the fact that during the high potential excursions the catalyst
314 experiences enhanced oxidation, independent of the reacting atmosphere. However,

315 applying the same procedures (i) and (iii) with the Pt/C catalyst with ca. 4-5 nm particle
316 size (TEC10E50E-HT), no influence of the reaction gas atmosphere on the recorded
317 ECSA loss is discernable, i.e. 19.2 ± 0.5 % in Ar and 18.2 ± 1.2 % in O_2 gas atmosphere.
318 The results therefore confirm previous reports stating that the gas atmosphere affects the
319 surface chemistry of the carbon supports [28, 45] but they also show that the influence
320 of the gas atmosphere on the ECSA losses is individually dependent on the Pt/C
321 catalyst.

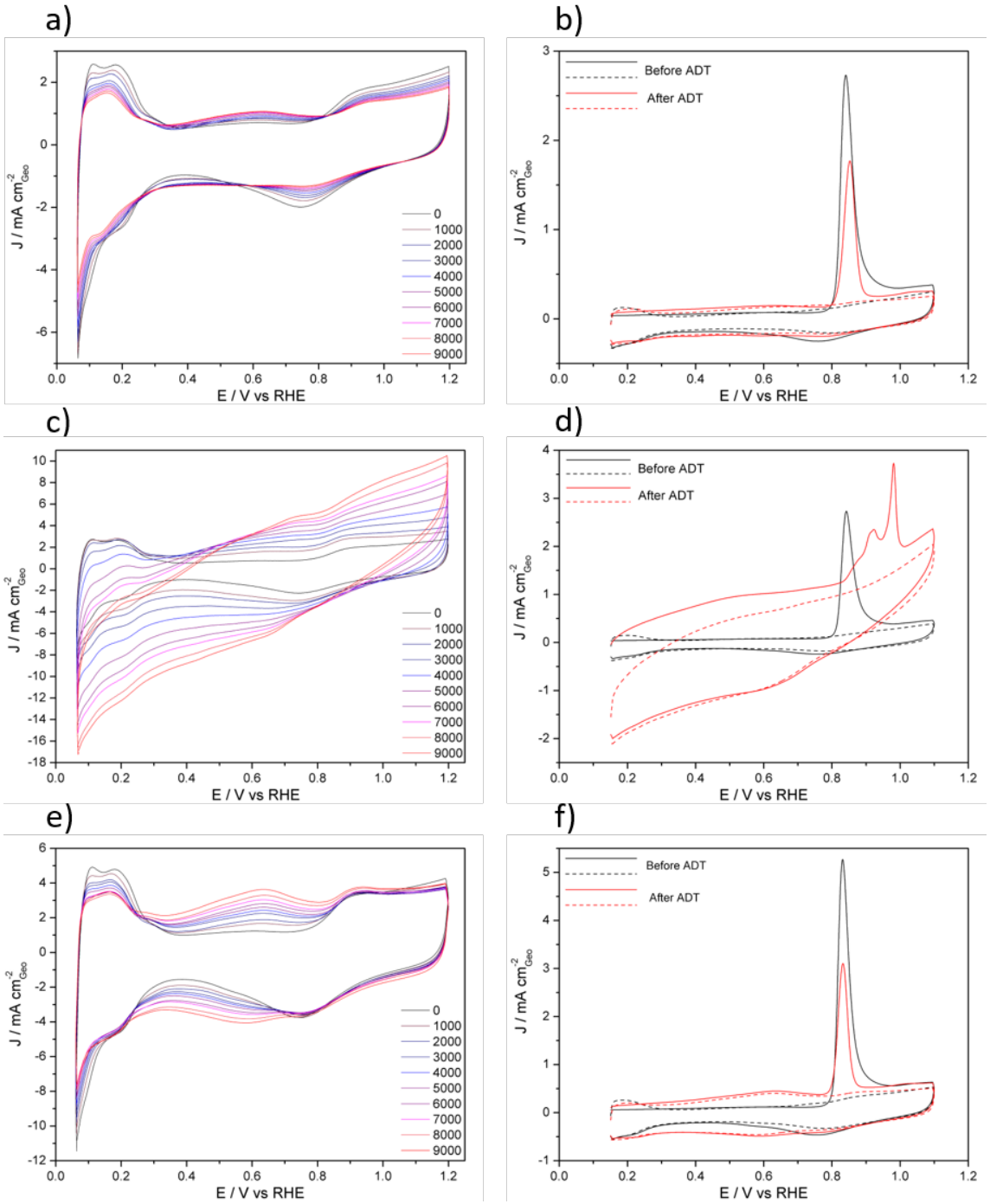

Figure 3. Influence of different ADT protocols performed in O_2 atmosphere on the electrochemical behavior of a commercial Pt/C catalyst (TEC10E50E). On the left-hand side, the cyclic voltammograms (sweep rate 0.5 V s^{-1}) recorded every 1000 cycles in Ar atmosphere are shown, whereas on the right-hand side the initial and final CO stripping curves (solid line) are shown together with the subsequent cyclic voltammogram (solid line); both recorded at a sweep rate of 0.05 V s^{-1}. (a,b) Step protocol simulating

load-cycles, (c,d) CV protocol simulating start-up/shutdown conditions, (e,f) Mixed protocol combining the two prior protocols. The measurements were performed at room temperature.

Table 1. The total loss in ECSA in % during the different ADT protocols as determined from the CO stripping measurements. The error is the standard deviation of three independent measurements.

ECSA loss / %				
Catalyst	Cell type	ADT protocol	Gas Atmosphere	
			Ar	O_2
TEC10E50E	Conventional cell	load-cycle protocol (i)	32.0 ± 1.6	37.2 ± 2.5
TEC10E50E	GDE cell	load-cycle protocol (i)	41.5 ± 2.3	48.1 ± 1.6
		mixed protocol (iii)	54.3 ± 0.1	57.4 ± 1.8
TEC10E50E-HT	GDE cell	load cycle protocol (i)	19.2 ± 0.5	18.2 ± 1.2
		mixed protocol (iii)	20.7 ± 0.4	24.0 ± 1.5

3.4. Influence of reactant gas humidity.

Another interesting factor for the degradation of PEMFC catalysts is the effect of the relative gas humidity. This factor is not accessible in standard electrochemical three-electrode setups with liquid aqueous electrolyte but can be easily studied in the GDE setup. To demonstrate the effect of the relative gas humidity, we performed a load cycle ADT in dry oxygen gas (protocol (i)). To be able to monitor the real loss in ECSA, before and after the ADT, CO stripping measurements were performed in humidified gas. The results are summarized in Figure 4. It is seen that in dry Argon gas, the H_{upd} region in the CVs – recorded as part of the load cycle protocol (i) – decreases indicating

a significant reduction in active Pt surface area. This sudden loss in active Pt surface area can be correlated to a significant deactivation in dry gas conditions. However, the final CV recorded under re-humidified conditions demonstrates that the active Pt surface area can to a large extend be recovered. That is, after applying the load cycle protocol (i) on the TEC10E50E Pt/C catalyst with a particle size of 2-3 nm, the ECSA loss in dry O_2 gas condition was ca. 50 %, whereas switching back to humidified O_2 gas, the overall ECSA loss is only ca. 28 %, which is less than applying the load cycle protocol (i) under fully humidified conditions.

The results can be interpreted in the following way. During the load cycle protocol (i), the active Pt surface area is significantly reduced due to a loss in proton conduction from the dry Nafion in the catalyst layer. Thus, only part of the catalyst is actually subjected to degradation while the other part remains unaltered. This results in an overall lower degradation when switching back to fully humidified conditions. Such behavior, however, is not expected in real PEMFC devices where the power output is decisive. In contrast to the potentiostatic ADT measurements, under amperometric conditions inaccessible Pt surface area due to dry gas conditions are expected to lead to increased degradation in the accessible part of the catalyst layer. To demonstrate this, we designed an amperometric ADT protocol that switches 600 times from load (i.e. 100 mA

cm^{-2}_{geo}) to open circuit potential (OCP) and back, holding the respective condition for 3 s each. Comparing the same TEC10E50E Pt/C catalyst under dry and humidified conditions, respectively, a significantly higher ECSA loss was observed for the dry O_2 gas (ca. 65 % loss) as compared to the humidified O_2 gas (ca. 10 % loss) conditions. In contrast to the potentiodynamic load cycle protocol (i), re-humidifying the catalyst after applying the amperometric ADT protocol, could only recover a small part of the ECSA (total loss of ca. 57 % instead of ca. 65 % loss)

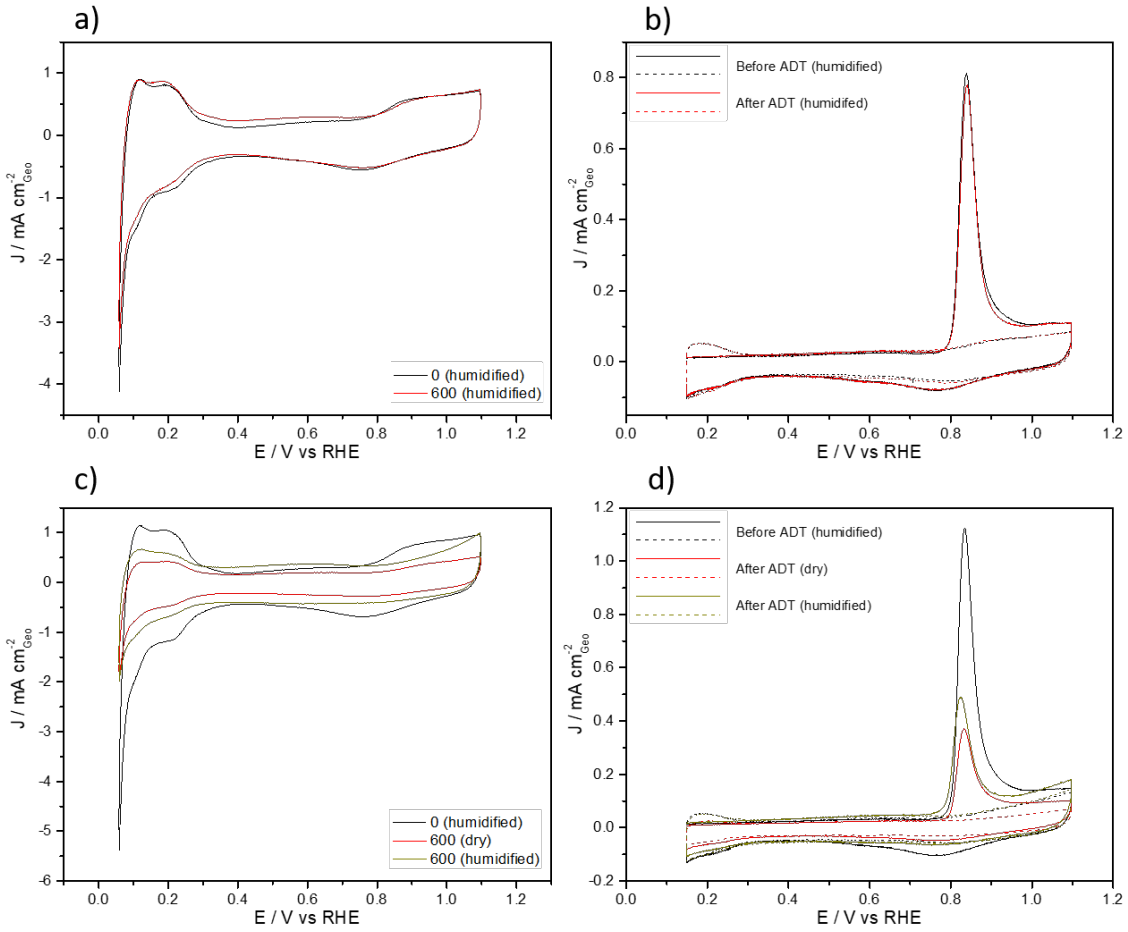

Figure 4. Influence of humidification of O_2 gas on the ECSA loss of a commercial Pt/C

376 catalyst (TEC10E50E) upon applying an amperometric ADT consisting of 600 steps
377 between load conditions (100 mA cm^{-2}_{geo}) and OCP, maintaining each condition for 3 s
378 each. (a,b) Cyclic voltammograms and CO stripping (sweep rate 0.05 V s^{-1}) before and
379 after ADT protocol applied under humidified O_2 gas. (c,d) Cyclic voltammograms and
380 CO stripping (sweep rate 0.05 V s^{-1}) before and after ADT protocol applied under dry
381 O_2 gas. The measurements before applying the ADT protocol were recorded under
382 humidified conditions. In addition, the effect of re-humidifying the O_2 gas after
383 applying the ADT protocol is shown. The measurements were performed at room
384 temperature.

385

386 *3. 5. IL-TEM measurements in GDE setup*

387 An advantage of half-cells with liquid electrolyte - as compared to MEA test - is the
388 possibility to perform IL-TEM measurements to analyze the degradation mechanism
389 leading to the loss in active surface area. Here, we demonstrate that the same is feasible
390 in the GDE setup and even elevated temperatures can be used, see Figure 5. By placing
391 the TEM grid between the membrane electrolyte and GDL, the IL-TEM method can be
392 applied straight forward. For the demonstration, a catalyst with lower Pt loading (20
393 wt. %) was used to facilitate the ability to follow the change of individual particles. The
394 typical degradation phenomena like migration and coalescence (yellow circles) and
395 particle detachment (red circle) can be clearly seen to occur as consequence of the
396 load-cycle treatment.

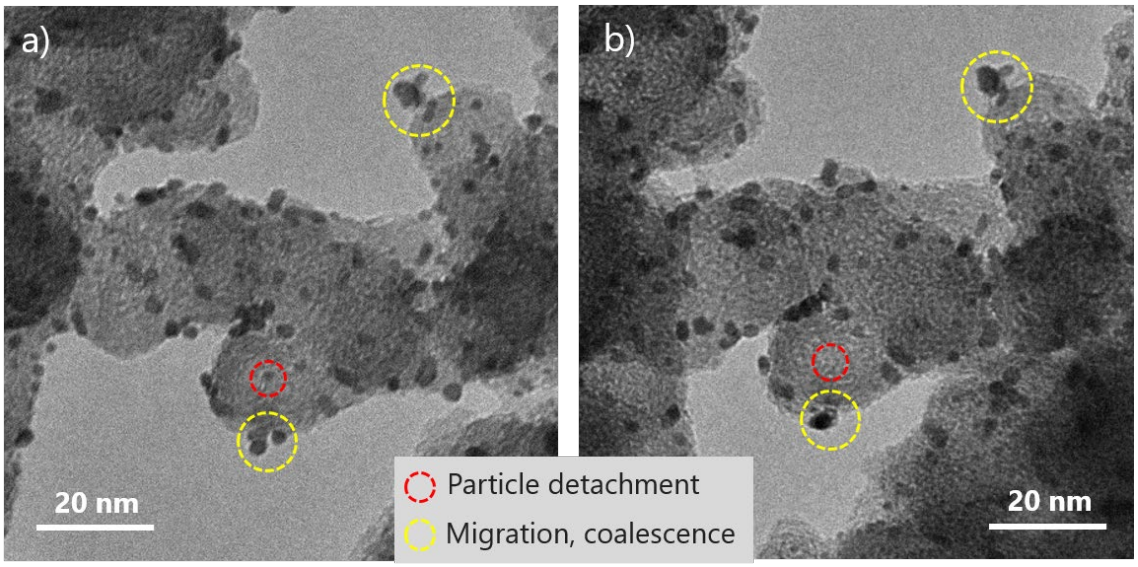

Figure 5. IL-TEM micrographs of a commercial 20 wt. % Pt/C catalyst (HiSPEC 3000) before and after load-cycle ADT treatment for 1200 cycles at 60 °C.

Conclusion

We demonstrate the application of our recently introduced gas diffusion electrode (GDE) setup for benchmarking the stability of PEMFC catalysts under realistic reaction conditions. It is shown that the popular ADT protocol proposed by the FCCJ to simulate load-cycle conditions leads to suitable results for describing the degradation behavior of the catalyst, whereas the protocol proposed for simulating start-up/shutdown conditions leads to massive corrosion of the carbon in the catalyst layer as well as MPL and GDL, thereby obstructing the ability to track the surface area loss of the catalyst. Therefore, we propose a combination of the two protocols limiting the number of high potential excursion as feasible alternative. Such treatment would also be closer to a realistic

411 condition, where not exclusively load-cycle or start-up/shutdown conditions are applied,
412 but both cases occur. Using these ADT protocols a significant influence of the particle
413 size on the ECSA loss is observed, although it is acknowledged that the (assumed) heat
414 treatment of the catalyst also changes the carbon support. Furthermore, it is shown that
415 the gas atmosphere (reactant or inert gas as well as dry or humidified gas) influences the
416 degradation behavior. In contrast to previous reports, it is demonstrated that the
417 influence of the presence of oxygen on the degradation depends on the ADT protocol
418 and the catalyst. No systematic difference between liquid and polymer environment was
419 seen, however, it is found that when applying high potential excursions, the influence of
420 reactant gas atmosphere gets less pronounced (for those cases where a clear influence is
421 observed).
422 More intriguing is the observed influence of the reactant humidity, which cannot be
423 studied in conventional cells using liquid electrolyte. It is found that under dry
424 conditions only parts of the catalyst layer participate in the reaction. In a potentiostatic
425 ADT protocol, almost all of the initial surface area can be re-established by switching
426 back to humidified conditions, i.e. the apparent loss in ECSA is reversible. This is,
427 however, not the case in a more realistic amperometric degradation protocol. This
428 finding highlights that to investigate such effects, additional ADT protocols are needed

to ensure that the entire catalyst layer is indeed participating the reaction.

Last but not least, it is demonstrated that the IL-TEM technique can easily integrated in the measurements allowing a combination of surface area loss determination and mechanistic insights. This is even possible at 60 °C, i.e. close to the actual operation temperature of a PEMFC. To sum up, it is demonstrated that the introduced GDE setup offers substantial advantages over standard degradation measurements in electrochemical cells employing liquid electrolyte.

Acknowledgments

This work was supported by the Swiss National Science Foundation (SNSF) via the project No. 200021_184742. M.I. and M.A. gratefully acknowledge support from Toyota Central R&D Labs., Inc. and J.S. the DFG for financial support (KU 3152/6-1).

References

1. Gasteiger, H.A., et al., *Activity benchmarks and requirements for Pt, Pt-alloy, and non-Pt oxygen reduction catalysts for PEMFCs.* Applied Catalysis B-Environmental, 2005. **56**(1-2): p. 9-35.
2. Borup, R., et al., *Scientific Aspects of Polymer Electrolyte Fuel Cell Durability and Degradation.* Chemical Reviews, 2007. **107**(10): p. 3904-3951.
3. Mayrhofer, K.J.J., et al., *Fuel cell catalyst degradation on the nanoscale.* Electrochemistry Communications, 2008. **10**(8): p. 1144-1147.
4. Hartl, K., M. Hanzlik, and M. Arenz, *IL-TEM investigations on the degradation mechanism of Pt/C electrocatalysts with different carbon supports.* Energy & Environmental Science, 2011. **4**(1): p. 234-238.
5. Mayrhofer, K.J.J., et al., *Non-destructive transmission electron microscopy study of catalyst degradation under electrochemical treatment.* Journal of Power Sources, 2008. **185**(2): p. 734-739.
6. Lafforgue, C., et al., *Degradation of Carbon-Supported Platinum-Group-Metal*

Electrocatalysts in Alkaline Media Studied by in Situ Fourier Transform Infrared Spectroscopy and Identical-Location Transmission Electron Microscopy. Acs Catalysis, 2019. **9**(6): p. 5613-5622.

7. Hodnik, N. and S. Cherevko, *Spot the difference at the nanoscale: identical location electron microscopy in electrocatalysis.* Current Opinion in Electrochemistry, 2019. **15**: p. 73-82.
8. Aran-Ais, R.M., et al., *Identical Location Transmission Electron Microscopy Imaging of Site-Selective Pt Nanocatalysts: Electrochemical Activation and Surface Disordering.* Journal of the American Chemical Society, 2015. **137**(47): p. 14992-14998.
9. Rasouli, S., et al., *Electrochemical Degradation of Pt-Ni Nanocatalysts: An Identical Location Aberration-Corrected Scanning Transmission Electron Microscopy Study.* Nano Letters, 2019. **19**(1): p. 46-53.
10. Souza, N.E., et al., *Support modification in Pt/C electrocatalysts for durability increase: A degradation study assisted by identical location transmission electron microscopy.* Electrochimica Acta, 2018. **265**: p. 523-531.
11. Lafforgue, C., et al., *Accelerated Stress Test of Pt/C Nanoparticles in an Interface with an Anion-Exchange Membrane-An Identical-Location Transmission Electron Microscopy Study.* Acs Catalysis, 2018. **8**(2): p. 1278-1286.
12. Kinumoto, T., et al., *Degradation of the Pt/C Electrode Catalyst Monitored by Identical Location Scanning Electron Microscopy during Potential Pulse Durability Tests in HClO4 Solution.* Electrochemistry, 2015. **83**(1): p. 12-17.
13. Schuppert, A.K., et al., *A Scanning Flow Cell System for Fully Automated Screening of Electrocatalyst Materials.* Journal of the Electrochemical Society, 2012. **159**(11): p. F670-F675.
14. Kasian, O., et al., *Electrochemical On-line ICP-MS in Electrocatalysis Research.* The Chemical Record, 2018. **19**: p. 2130-2142.
15. Pizzutilo, E., et al., *On the Need of Improved Accelerated Degradation Protocols (ADPs): Examination of Platinum Dissolution and Carbon Corrosion in Half-Cell Tests.* Journal of the Electrochemical Society, 2016. **163**(14): p. F1510-F1514.
16. Marcu, A., et al., *Ex situ testing method to characterize cathode catalysts degradation under simulated start-up/shut-down conditions - A contribution to polymer electrolyte membrane fuel cell benchmarking.* Journal of Power Sources, 2012. **215**: p. 266-273.

17. Borup, R.L., et al., *PEM fuel cell electrocatalyst durability measurements.* Journal of Power Sources, 2006. **163**(1): p. 76-81.
18. Ohma, A., et al., ECS Transactions, 2011. **41**(1): p. 775-784.
19. Park, Y.-C., et al., Electrochimica Acta, 2013. **91**(0): p. 195-207.
20. Zana, A., et al., *Probing Degradation by IL-TEM: The Influence of Stress Test Conditions on the Degradation Mechanism.* Journal of the Electrochemical Society, 2013. **160**(6): p. F608-F615.
21. Ferreira, P.J., et al., *Instability of Pt/C electrocatalysts in proton exchange membrane fuel cells - A mechanistic investigation.* Journal of the Electrochemical Society, 2005. **152**(11): p. A2256-A2271.
22. Kucernak, A.R. and E. Toyoda, *Studying the oxygen reduction and hydrogen oxidation reactions under realistic fuel cell conditions.* Electrochemistry Communications, 2008. **10**(11): p. 1728-1731.
23. Fleige, M., et al., *Evaluation of temperature and electrolyte concentration dependent Oxygen solubility and diffusivity in phosphoric acid.* Electrochimica Acta, 2016. **209**: p. 399-406.
24. Fleige, M.J., G.K.H. Wiberg, and M. Arenz, *Rotating disk electrode system for elevated pressures and temperatures.* Review of Scientific Instruments, 2015. **86**(6).
25. Wiberg, G.K.H., M.J. Fleige, and M. Arenz, *Design and test of a flexible electrochemical setup for measurements in aqueous electrolyte solutions at elevated temperature and pressure.* Review of Scientific Instruments, 2014. **85**(8).
26. Pinaud, B.A., et al., *Key Considerations for High Current Fuel Cell Catalyst Testing in an Electrochemical Half-Cell.* Journal of the Electrochemical Society, 2017. **164**(4): p. F321-F327.
27. Zalitis, C.M., D. Kramer, and A.R. Kucernak, *Electrocatalytic performance of fuel cell reactions at low catalyst loading and high mass transport.* Physical Chemistry Chemical Physics, 2013. **15**(12): p. 4329-4340.
28. Nikkuni, F.R., et al., *The role of water in the degradation of Pt3Co/C nanoparticles: An Identical Location Transmission Electron Microscopy study in polymer electrolyte environment.* Applied Catalysis B-Environmental, 2014. **156**: p. 301-306.
29. Zalitis, C.M., et al., *Properties of the hydrogen oxidation reaction on Pt/C catalysts at optimised high mass transport conditions and its relevance to the anode reaction in PEFCs and cathode reactions in electrolysers.* Electrochimica

Acta, 2015. **176**: p. 763-776.
30. Wiberg, G.K.H., M. Fleige, and M. Arenz, *Gas diffusion electrode setup for catalyst testing in concentrated phosphoric acid at elevated temperatures.* Review of Scientific Instruments, 2015. **86**(2).
31. Inaba, M., et al., *Benchmarking high surface area electrocatalysts in a gas diffusion electrode: measurement of oxygen reduction activities under realistic conditions.* Energy & Environmental Science, 2018. **11**(4): p. 988-994.
32. Sievers, G.W., et al., *Sputtered Platinum Thin-films for Oxygen Reduction in Gas Diffusion Electrodes: A Model System for Studies under Realistic Reaction Conditions.* Surfaces, 2019. **2**(2): p. 336-348.
33. Higgins, D., et al., *Gas-Diffusion Electrodes for Carbon Dioxide Reduction: A New Paradigm.* ACS Energy Letters, 2019. **4**(1): p. 317-324.
34. Wiberg, G.K.H., K.J.J. Mayrhofer, and M. Arenz, *Investigation of the Oxygen Reduction Activity on Silver - A Rotating Disc Electrode Study.* Fuel Cells, 2010. **10**(4): p. 575-581.
35. Reiser, C.A., et al., *A Reverse-Current Decay Mechanism for Fuel Cells.* Electrochemical and Solid-State Letters, 2005. **8**(6): p. A273-A276.
36. Kangasniemi, K.H., D.A. Condit, and T.D. Jarvi, *Characterization of Vulcan Electrochemically Oxidized under Simulated PEM Fuel Cell Conditions.* Journal of The Electrochemical Society, 2004. **151**(4): p. E125-E132.
37. Speder, J., et al., *On the influence of the Pt to carbon ratio on the degradation of high surface area carbon supported PEM fuel cell electrocatalysts.* Electrochemistry Communications, 2013. **34**: p. 153-156.
38. Topalov, A.A., et al., *The impact of dissolved reactive gases on platinum dissolution in acidic media.* Electrochemistry Communications, 2014. **40**: p. 49-53.
39. Cheah, S.K., et al., *CO Impact on the Stability Properties of PtxCoy Nanoparticles in PEM Fuel Cell Anodes: Mechanistic Insights.* Journal of the Electrochemical Society, 2011. **158**(11): p. B1358-B1367.
40. Franco, A.A., et al., *Impact of carbon monoxide on PEFC catalyst carbon support degradation under current-cycled operating conditions.* Electrochimica Acta, 2009. **54**(22): p. 5267-5279.
41. Zana, A., et al., *Investigating the corrosion of high surface area carbons during start/stop fuel cell conditions: A Raman study.* Electrochimica Acta, 2013. **114**: p. 455-461.
42. Schlogl, K., M. Hanzlik, and M. Arenz, *Comparative IL-TEM Study Concerning*

the Degradation of Carbon Supported Pt-Based Electrocatalysts. Journal of the Electrochemical Society, 2012. **159**(6): p. B677-B682.

43. Makharia, R., et al., *Durable PEM Fuel Cell Electrode Materials: Requirements and Benchmarking Methodologies.* ECS Transactions, 2006. **1**(8): p. 3-18.

44. Speder, J., et al., *Pt based PEMFC catalysts prepared from colloidal particle suspensions – a toolbox for model studies.* Physical Chemistry Chemical Physics, 2013. **15**(10): p. 3602-3608.

45. Castanheira, L., et al., *Carbon Corrosion in Proton-Exchange Membrane Fuel Cells: Effect of the Carbon Structure, the Degradation Protocol, and the Gas Atmosphere.* Acs Catalysis, 2015. **5**(4): p. 2184-2194.